

Density profiles of an imbalance trapped Fermi gas near a Feshbach resonance

Theja N. De Silva^{a,b}, Erich J. Mueller^a

^a LASSP, Cornell University, Ithaca, New York 14853, USA.

^b Department of physics, University of Ruhuna, Matara, Sri Lanka.

We investigate the density profiles of a partially polarized trapped Fermi gas in the BCS-BEC crossover region using mean field theory within the local density approximation. Within this approximation the gas is phase separated into concentric shells. We describe how the structure of these shells depends upon the polarization and the interaction strength. Comparison with experiments yields insight into the possibility of a polarized superfluid phase.

INTRODUCTION

Advances in the trapping and manipulating of degenerate Fermi atoms are attracting intense interest from physicists in the fields of condensed matter physics, atomic molecular and optical physics, nuclear physics, astrophysics and particle physics. Current and future experiments aim to use this highly controlled environment to explore many-body phenomena with impact on widely varying areas of physics. We discuss the theory of one such set of phenomena; the properties of trapped partially polarized fermionic atoms, where the two spin states have different Fermi surfaces.

The study of Fermi systems with mismatched Fermi surfaces began with attempts by Fulde and Ferrell, and Larkin and Ovchinnikov (FFLO)[1] to understand magnetized superconductors. More recent work has come from researches in the nuclear physics community who are studying superconductivity in nuclear matter and quark matter, with possible application to neutron stars or heavy ion collisions [2]. Such calculations have taken on new relevance with the possibility of cold gas experiments where alkali atoms are trapped in a number of distinguishable hyperfine states, with negligible spin relaxation. Thus one can produce a two-component Fermi gas with arbitrary population imbalance. Using magnetic-field driven Feshbach resonances [3], the interactions between these atoms can be made large enough to drive the system superfluid.

Very recently, there have been two experimental studies of trapped ${}^6\text{Li}$ Fermi atoms with mismatched Fermi surfaces[4, 5]. By analyzing time-of-flight images, Zwierlein *et al.* [4] found evidence for phase separation between regions of equal and unequal population density. Furthermore by studying vortices, they were able to monitor the evolution of superfluidity as a function of population imbalance: finding not only that polarization inhibits superfluidity, but that the superfluid region appears to coincide with the region of equal density. The equally exciting work of Partridge *et al.* [5] directly shows phase separation through high resolution *in-situ* images of the atomic clouds.

In this paper, we study the density profile in the entire

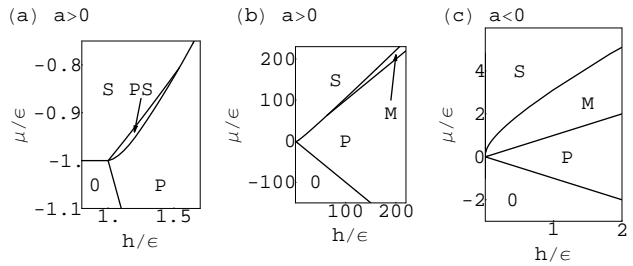


FIG. 1: Mean-field phase diagram of homogeneous two component Fermi gas in the (a), (b) BEC and (c) BCS regimes. Phases only depend on the dimensionless ratio of the chemical potentials $\mu = (\mu_\uparrow + \mu_\downarrow)/2$ and $h = (\mu_\uparrow - \mu_\downarrow)/2$, and the energy scale of the interactions, $\epsilon = \hbar^2/2ma^2$.

BCS-BEC crossover region within mean field theory. We use a local density approximation (LDA) and compare our results with experiments. Our study shows that the population imbalanced trapped Fermi gas is generically phase separated into concentric shells. Within our approximations, each region of space can be in one of several phases: unpolarized superfluid (S), polarized superfluid (PS), normal mixture (M), or fully polarized normal (P). The unpolarized superfluid coincides with the standard equal-population superfluid predicted by the BCS-BEC crossover theory [6, 7, 8, 9, 10]. The polarized superfluid, which in mean-field theory is only found on the BEC side of resonance, consists of an interpenetrating gas of bosonic atoms and a fully polarized gas of fermions [11, 12]. The normal mixture and fully polarized normal phases both lack superfluidity and are distinguished by the presence or absence of the minority species of fermion. Due to the extremely small portion of the phase diagram where it is expected to appear, we do not consider the possibility of an inhomogeneous FFLO phase. As seen in the recent work by Sheehy *et al.* [11] and the Bogoliubov-deGennes calculation of Kinnunen *et al.* [13], such a phase would appear on the BCS side of resonance as subtle structure in the domain wall separating the S and M regions.

We find three different parameter regimes, distinguished by the structure of these shells: (1) BCS regime where $(k_f a)^{-1} \lesssim 0$, (2) Crossover-BEC regime where

$0 \lesssim (k_f a)^{-1} \lesssim 1$ and (3) Deep-BEC regime where $(k_f a)^{-1} \gtrsim 1$. The Fermi wavevector is k_f and the scattering length is a . Depending upon density and polarization, regime (1) contains two scenarios – from center to edge one finds S-M-P or M-P. In regime (2) one finds S-P at small polarizations and S-M-P or M-P for larger. In regime (3) one finds S-PS-P for small polarizations and PS-P for larger polarizations [14]. In an appropriately defined thermodynamic limit there is a quantum phase transition between each of these possibilities as one varies the parameters of the system. This behavior should be contrasted with the smooth crossover physics found in the absence of a population imbalance.

Our results are consistent with the experiments reported in ref. [4], however, due to the expansion procedure used in those experiments no quantitative comparison can be made. We find partial agreement with the experiments reported in ref. [5]. In particular, for sufficiently large polarizations we reproduce the values of the axial radius of the superfluid core and the outer edge of the gas cloud found in the experiments. Our total density profile also closely agrees with the experiment. However, we find that the spatial structure of the difference between up and down spins differ significantly from those found in the experiment. We demonstrate that this discrepancy points to either unexpectedly large anharmonicities or an unexplained breakdown of the local density approximation. In fact we show that despite the large ratio of the trap size to the coherence length, the experimental data is inconsistent with any LDA that assumes a harmonic trap, regardless of the equation of state used.

The most significant open theoretical question at the moment is the possibility of a polarized superfluid region at unitarity (UPS). The mean-field calculation unambiguously predicts that such a region does not exist. Monte-Carlo calculations suggest that such a region may exist, but are currently not conclusive [15]. Based upon comparison with our mean-field calculations we argue that the experimental measure of phase separation (from analyzing the density profiles) is slightly ambiguous and one may be able to explain the experiments without recourse to a UPS. On the other hand, the poor agreement in the radii at small polarizations may support the notion of a UPS.

Concurrent with the preparation of this manuscript, Pieri *et al.* [16], Kinnunen *et al.* [13], Yi *et al.* [17], Chevy [18], and Caldas[19] presented theoretical studies of the effect of trap potentials on a partially polarized gas. These works complement our own. Pieri *et al.* gives a quite thorough discussion of the formal underpinnings of the approximations which we use, and produce similar density profiles on the BEC side of resonance. Kinnunen *et al.* go beyond the local density approximation, and are able to produce both density profiles and RF-spectra for relatively small numbers of particles on the BCS side

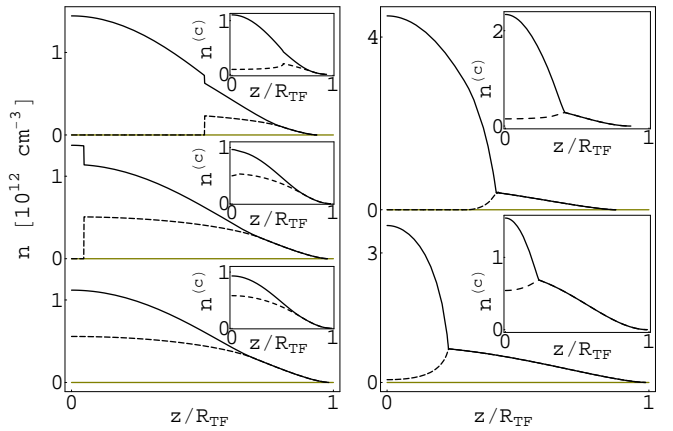


FIG. 2: On-axis mean-field density profiles $n(z, \rho = 0)$ of zero temperature harmonically trapped partially polarized Fermi gas, illustrating all of the cases described in the text. Solid lines show total density $n_\uparrow + n_\downarrow$, while dashed lines show density differences $n_\uparrow - n_\downarrow$. Left (right) figures represent BCS (BEC) regime with $k_f a = -2, (0.5)$. The Thomas-Fermi radius is defined as $R_{TF} = \sqrt{(2\epsilon_f)/(m\omega_z^2)}$, where $\epsilon_f = \hbar^2 k_f^2/2m = \hbar\bar{\omega}(6N)^{1/3}$ with average trap frequency $\bar{\omega} = (\omega_\perp^2 \omega_z)^{1/3}$. Inset shows column density $n^{(c)} = \int d\rho n(z, \rho)$ measured in units of $[10^9 \text{ cm}^{-2}]$. All graphs use $N_\uparrow + N_\downarrow = 2 \times 10^5$ atoms in an axial symmetric trap with $\omega_z = 2\pi \times 7.2 \text{ Hz}$, and $\omega_\perp = 2\pi \times 350 \text{ Hz}$. BCS figures (top to bottom) have polarizations $P = (N_\uparrow - N_\downarrow)/(N_\uparrow + N_\downarrow) = 0.30, 0.74, 0.80$ and BEC figures have $P = 0.33, 0.90$.

of resonance. The similarity of our results with those of Kinnunen *et al.* lends us additional confidence in our approach. Yi *et al.* study the phase separation using minimization of the thermodynamic potential. Chevy uses universality to study the density profile at unitarity while Caldas investigates the stability of the phases by comparing the surface energies between the normal and superfluid components.

Prior theoretical work on superfluidity with mismatched Fermi surfaces has been restricted to either homogeneous systems [11, 12, 20, 21, 22] or trapped systems in the weakly coupling limit [24].

FORMALISM

We restrict ourselves to the wide resonance of ${}^6\text{Li}$ where both of the available experiments [4, 5] have been carried out, and therefore we do not need to explicitly consider the closed channel of the Feshbach resonance. The fermions of different hyperfine states \uparrow and \downarrow interact through a short-range effective potential $-u\delta(\vec{r}' - \vec{r})$. The system of $N = N_\uparrow + N_\downarrow$ atoms is then described by the Hamiltonian [7, 8, 9] $H = H_1 + H_2$, with $H_1 = \sum_\sigma \int d^3\vec{r} \psi_\sigma^\dagger(\vec{r}) [-\frac{\hbar^2 \nabla^2}{2m} - \mu_0 \sigma + V(\vec{r})] \psi_\sigma(\vec{r})$ containing kinetic and trapping energies and

$H_2 = -u \int d^3 \vec{r} \psi_\uparrow^\dagger(\vec{r}) \psi_\downarrow^\dagger(\vec{r}) \psi_\downarrow(\vec{r}) \psi_\uparrow(\vec{r})$ containing interactions. The field operators $\psi_\sigma(\vec{r})$ obey the usual fermionic anticommutation rules, and describe the annihilation of a fermion at position \vec{r} in the hyperfine state σ . Parameters m , $\mu_{0\sigma}$ and $V(\vec{r}) = \frac{1}{2}m(\omega_\perp^2 \rho^2 + \omega_z^2 z^2)$ are the mass, chemical potential and trapping potential of the atomic species σ . We introduce a local chemical potential $\mu_\sigma(\vec{r}) = \mu_{0\sigma} - V(\vec{r})$ and treat the system as locally homogeneous. Without loss of generality, we take \uparrow to be the majority species of atoms and describe the system in terms of the spatially independent chemical potential difference $h = (\mu_\uparrow - \mu_\downarrow)/2 \geq 0$, and the spatially dependent average chemical potential $\mu(\vec{r}) = (\mu_\uparrow + \mu_\downarrow)/2$. Using the usual BCS mean field decoupling, the BCS-Bogoliubov excitation spectrum of each species is given by $E_{k\sigma}(\vec{r}) = \xi_\sigma h + \sqrt{(\epsilon_k - \mu)^2 + \Delta^2}$. Here $\epsilon_k = \hbar^2 k^2/2m$ is the kinetic energy, $\Delta(\vec{r}) = u \langle \psi_\downarrow(\vec{r}) \psi_\uparrow(\vec{r}) \rangle$ is the local superfluid order parameter, and $\xi_\uparrow = -1$ and $\xi_\downarrow = +1$.

At zero temperature, the gap $\Delta(\vec{r})$ and the the number densities $n(\vec{r}) = n_\uparrow(\vec{r}) + n_\downarrow(\vec{r})$, $n_d(\vec{r}) = n_\uparrow(\vec{r}) - n_\downarrow(\vec{r})$ satisfy

$$\begin{aligned} \frac{-m}{2\pi\hbar^2 a} &= \int_0^\infty \frac{d^3 \vec{k}}{(2\pi)^3} \left(\frac{1}{E_k} - \frac{1}{\epsilon_k} \right) - \int_{k_-}^{k_+} \frac{d^3 \vec{k}}{(2\pi)^3} \frac{1}{E_k} \quad (1) \\ n(\vec{r}) &= \int_0^\infty \frac{d^3 \vec{k}}{(2\pi)^3} \left(1 - \frac{\epsilon_k - \mu}{E_k} \right) + \int_{k_-}^{k_+} \frac{(\epsilon_k - \mu)}{E_k} \quad (2) \\ n_d(\vec{r}) &= \frac{1}{(2\pi)^3} \frac{4\pi}{3} (k_+^3 - k_-^3). \quad (3) \end{aligned}$$

We define $E_k(\vec{r}) = (E_{k\uparrow} + E_{k\downarrow})/2$, and $k_\pm(\vec{r}) = (\pm\sqrt{h^2 - \Delta^2} + \mu)^{1/2}$. The ultraviolet divergence associated with the delta-function interaction has been eliminated [7, 8, 10, 25] by introducing the effective scattering length through $-m/(4\pi\hbar^2 a) = u^{-1} - \int_0^\infty d^3 \vec{k} (2\pi)^{-3} / 2\epsilon_k$. Notice that $n_d(\vec{r})$ is non-zero as long as $h > \Delta$ and $\mu > -\sqrt{h^2 - \Delta^2}$.

At each point in space one finds Δ by solving equation (1) at fixed μ and h . As a nonlinear equation, there are multiple solutions – some of which correspond to energy minima, some to saddle points. For example, the Sarma states [21, 22, 23] appear as saddle points. We take the lowest energy solution, producing the phase diagram illustrated in figure 1. Within the cloud h is uniform, while μ varies monotonically from the center to edge of the cloud. The configurations of local phases, as described in the introduction, are found by following vertical lines in the figure. One determines μ_0 and h by imposing a constraint on the total number of particles $N = \int d^3 \vec{r} n(\vec{r})$ and the polarization $P = (N_\uparrow - N_\downarrow)/N$. Typical density profiles are shown in figure 2. Evolution of the radii of phase boundaries are shown in figure 5.

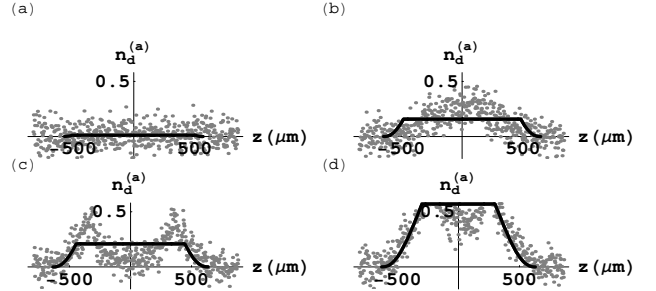


FIG. 3: Axial density difference $n_d^{(a)}(z) = 2\pi \int d\rho \rho [n_\uparrow(z, \rho) - n_\downarrow(z, \rho)]$ of zero temperature harmonically trapped partially polarized Fermi gas in units of $[10^6 \text{ cm}^{-1}]$. Figures (a), (b), (c), and (d) represent polarization $P = 0.01$, 0.09 , 0.14 , and 0.53 respectively. All graphs use the experimental parameters from reference [5] and the grey points are the experimental data.

EXPERIMENTS

There are profound differences in the full three-dimensional density profile of the experimental cloud and our predictions. These differences are best seen by looking at the *axial* density profile $n_d^{(a)}(z) = 2\pi \int d\rho \rho n_d(z, \rho) = \int dy n_d^{(c)}(z, y=0)$, found by integrating the two-dimensional column density over the y -direction. As shown in figure 3, we find a monotonic axial profile, while at polarizations above $P \approx 0.1$, Partridge *et al.* experimentally see a non monotonic density difference, with a dip in the center and horns on the edges. Despite these horns, our calculation of the total axial density $n^{(a)}(z) = 2\pi \int d\rho \rho n(z, \rho)$ agrees extremely well with the experimental data (FIG. 4).

Assuming LDA in a harmonic trap, the density is only a function of $\mu(r) = \mu_0 - m\omega_\perp^2 \rho^2/2 - m\omega_z^2 z^2/2$. One can therefore write $n_d^{(a)}(z) = \frac{2\pi}{m\omega_\perp^2} f(\mu_0 - m\omega_z^2 z^2/2)$, where $f(\bar{\mu}) = \int_{-\infty}^{\bar{\mu}} d\mu n_d(\mu)$. Since $n_d > 0$ one has $f(\bar{\mu})$ is monotonic and $n_d^{(a)}(z)$ must decrease monotonically as z increases from 0. In other words the horns seen in the experimental density differences are not consistent with the LDA. This result is based solely on the local density approximation and harmonic trapping – it does not require mean field theory.

Even if mean field theory breaks down, these experiments should be well described by a local density approximation. The only relevant microscopic scale near unitary is the Fermi temperature $T_f \approx 400 \text{ nK}$, which is over 20 times larger than the quantization scale of the harmonic trap $\hbar\omega_\perp/k_B \approx 17 \text{ nK}$, which is a characteristic scale for density variations. The simplest explanation for the discrepancy would be that anharmonicities in the optical trap are modifying the density profile, though we cannot rule out more exotic possibilities.

Further experimental and theoretical work is needed to

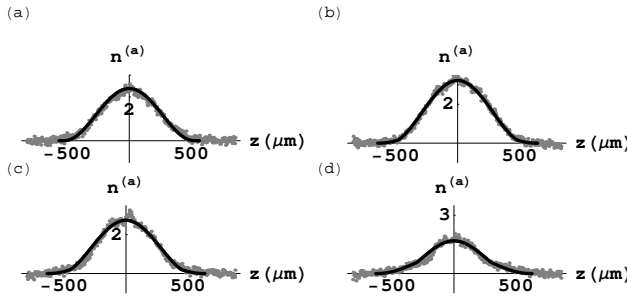


FIG. 4: Comparison of the axial density $n^{(a)}(z) = 2\pi \int d\rho \rho [n_{\uparrow}(z, \rho) + n_{\downarrow}(z, \rho)]$ with experimental data of reference [5]. Labels are the same as those of figure 3.

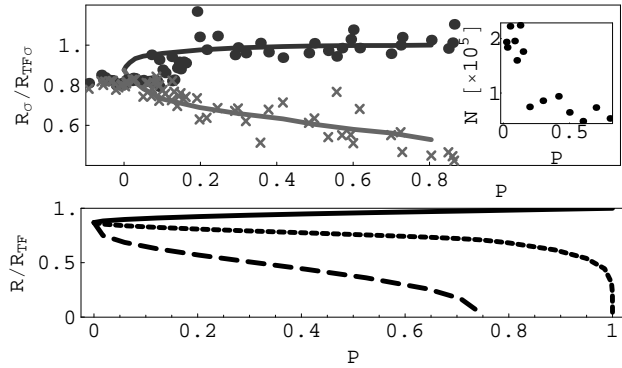


FIG. 5: TOP: Radii of the minority and majority components using experimental parameters from reference[5]. Dots and crosses are the experimental data for the majority and minority components respectively. Lines show our theoretical predictions. Inset shows the total number of atoms used for calculation at each P . The two spin state radii ($R_{\uparrow}, R_{\downarrow}$) are separately scaled by $R_{TF\uparrow}$ and $R_{TF\downarrow}$, where $R_{TF\sigma}$ is the Thomas-Fermi radius of a noninteracting one-component cloud with N_{σ} atoms. BOTTOM: Radii of phase boundaries in the BCS regime with $k_f a = -2$. Solid, short-dashed, and long-dashed lines are the boundaries of polarized normal, normal mixture, and unpolarized superfluid. Input parameters are the same as those of figure 2, as is the definition of R_{TF} .

settle this issue. It is particularly important because Partridge *et al.* interpret the appearance of horns as a transition between a unitary polarized superfluid and a phase separation between superfluid and normal regions. Since the LDA predicts that the horns do not exist in a phase separated cloud, we caution strongly against taking their disappearance as evidence for a polarized superfluid.

ACKNOWLEDGMENTS

This work was supported by NSF grant PHY-0456261, and by the Sloan Foundation. We are grateful to R. Hulet and W. Li for very enlightening discussions, and for sending us the data in figures 3, 4 and 5. We thank D.

E. Sheehy and L. Radzihovsky for the critical comments on the manuscript.

[1] P. Fulde and R. A. Ferrell, Phys. Rev. **135**, A550 (1964) and A.I. Larkin and Yu.N. Ovchinnikov, Zh. Eksp. Teor. Fiz. 47, 1136 (1964) [Sov. Phys. JETP 20, 762 (1965)].

[2] A. Sedrakian and U. Lombardo, Phys. Rev. Lett. **84**, 602 (2000); J. A. Bowers and K. Rajagopal, Phys. Rev. D **66**, 065002 (2002); I. Shovkovy and M. Huang, Phys. Lett. B **564**, 205 (2003); R. Casalbuoni and G. Nardulli, Rev. Mod. Phys. 76, 263 (2004).

[3] H. Feshbach, Ann.Phys. **19**, 287 (1962).

[4] Martin W. Zwierlein, Andr Schirotzek, Christian H. Schunck, Wolfgang Ketterle, Science Express, Published online, December 22 2005.

[5] Guthrie B. Partridge, Wenhui Li, Ramsey I. Kamar, Yean-an Liao, and Randall G. Hulet, Science Express, Published online, December 23 2005.

[6] A. J. Leggett, in Modern Trends in the Theory of Condensed Matter, edited by A. Pekalski and R. Przystawa (Springer-Verlag, Berlin, 1980); P. Nozieres and S. Schmitt-Rink, J. Low Temp. Phys. **59**, 195 (1985); D. M. Eagles, Phys. Rev. **186**, 456 (1969); A. Tokumitsu, K. Miyake and, K. Yamada, Phys. B **47**, 11988 (1993); J. R. Engelbrecht, M. Randeria and C. A. R. Sa de Melo, Phys. Rev. B **55**, 15153 (1997).

[7] Y. Ohashi and A. Griffin, Phys. Rev. Lett. **89**, 130402 (2002).

[8] J. N. Milstein, S. J. J. M. F. Kokkelmans, and M. J. Holland, Phys. Rev. A **66**, 043604 (2002).

[9] E. Timmermans, K. Furuya, P. W. Milonni, and A. K. Kerman, Phys. Lett. A **285**, 228 (2001); M. Holland, S. J. M. F. Kokkelmans, M. L. Chiofalo, and R. Walser, Phys. Rev. Lett. **87**, 120406 (2001); A. Perali, P. Pieri, and, G. C. Strinati, Phys. Rev. A **68**, 031601(R) (2003); T. Kostyrko and J. Ranninger, Phys. Rev. B **54**, 13105 (1996).

[10] C.A.R. S de Melo, M. Randeria, and J.R. Engelbrecht, Phys. Rev. Lett. **71**, 3202 (1993); Y. Ohashi and A. Griffin, Phys. Rev. A **67**, 033603 (2003); Y. Ohashi and A. Griffin, Phys. Rev. A **67**, 063612 (2003).

[11] D.E. Sheehy and L. Radzihovsky, cond-mat/0508430.

[12] C.-H. Pao, Shin-TzaWu, and S.-K. Yip, cond-mat/0506437.

[13] J. Kinnunen, L. M. Jensen, and P. Torma, preprint, cond-mat/0512556.

[14] This PS-P shell structure was discussed in reference [11].

[15] J. Carlson and S. Reddy, Phys. Rev. Lett. **95**, 060401 (2005).

[16] P. Pieri, and G.C. Strinati, preprint, cond-mat/0512354.

[17] W. Yi, and L. -M. Duan, preprint, cond-mat/0601006.

[18] F. Chevy, preprint, cond-mat/0601122.

[19] H. Caldas, preprint, cond-mat/0601148.

[20] R. Combescot, Europhys. Lett. **55**, 150 (2001); H. Caldas, Phys. Rev. A **69**, 063602 (2004); A. Sedrakian, J. Mur-Petit, A. Polls; H. Muther, Phys. Rev. A **72**, 013613 (2005); U. Lombardo, P. Nozières, P. Schuck, H.-J. Schulze, and A. Sedrakian, Phys. Rev. C **64**, 064314 (2001); D.T. Son and M.A. Stephanov, cond-mat/0507586; L. He, M. Jin and P. Zhuang, cond-

mat/0601147.

[21] W.V. Liu and F. Wilczek, Phys. Rev. Lett. **90**, 047002 (2003).

[22] P. F. Bedaque, H. Caldas, and G. Rupak, Phys. Rev. Lett. **91**, 247002 (2003).

[23] G. Sarma, J. Phys. Chem. Solids **24**, 1029 (1963).

[24] T. Mizushima, K. Machida, and M. Ichioka, Phys. Rev. Lett. **94**, 060404 (2005); P. Castorina, M. Grassò, M. Oertel, M. Urban, and D. Zappal'a, Phys. Rev. A **72**, 025601 (2005).

[25] S.J.J.M.F. Kokkelmans, J.N. Milstein, M.L. Chiofalo, R. Walser, and M.J. Holland, Phys. Rev. A **65**, 053617 (2002).